Oxygen storage capacity and thermal stability of brownmillerite-type Ca$_2$(Al$_{1-x}$Ga$_x$)MnO$_{5+\delta}$ oxides

Xiubing Huang,[a,b]* Chengsheng Ni,[b,c] John T.S. Irvine*[b]

[a] *Beijing Key Laboratory of Function Materials for Molecule & Structure Construction, School of Materials Science and Engineering, University of Science and Technology Beijing, Beijing, 100083, China*

[b] *School of Chemistry, University of St Andrews, St Andrews, KY16 9ST, Scotland, UK*

[c] *College of Resources and Environment, Southwest University, Beibei, Chongqing, 400716, China*

* Email: xiubinghuang@ustb.edu.cn (Dr. Xiubing Huang), jtsi@st-andrews.ac.uk (Prof. John T.S. Irvine)

Abstract

Understanding the oxygen uptake/release mechanism in oxygen storage materials is of great importance in the design of energy-related materials and their corresponding applications. In this work, the effects of Ga doping amount on the oxygen storage capacity and thermal stability of $Ca_2(Al_{1-x}Ga_x)MnO_{5+\delta}$ $(0 \leq x \leq 1)$ with a brownmillerite-type structure were investigated. $Ca_2AlMnO_{5+\delta}$ can reversibly store/release a large amount of excess oxygen (~3.0 wt%) at low temperature (between 300 and 600 ℃) under oxidative atmospheres. With the increasing Ga doping amount in $Ca_2(Al_{1-x}Ga_x)MnO_{5+\delta}$, these materials uptake less oxygen at higher temperature which can be attributed to the difficulty in the oxidation of tetrahedral GaO_4 blocks into octahedral GaO_6 blocks under 1 atm O_2. However, with the increasing of Ga-substitution amount, these $Ca_2(Al_{1-x}Ga_x)MnO_{5+\delta}$ $(0 \leq x < 1)$ can start to uptake oxygen at lower temperatures during the cooling process under flowing O_2 due to the distorted structure. The results demonstrated that $Ca_2(Al_{1-x}Ga_x)MnO_{5+\delta}$ $(0 \leq x < 1)$ can reversibly store/release large amounts of oxygen via just controlling the surrounding temperature and/or oxygen partial pressure but without using reductive gases, which would enable them great potentials in many applications.

Keywords: Oxygen storage materials; brownmillerite-type structure; Doping effect; Reversible behaviour

1. Introduction

Metal oxides based on valence-changeable constituent cations have the ability to exhibit oxygen nonstoichiometry, which is often related to oxygen uptake/release capacity.[1-4] Those oxides with remarkable oxygen uptake/release capability can be regarded as oxygen storage materials (OSMs), but excellent OSMs should also possess some other properties, such as quick and reversible adsorption/desorption of oxygen controlled by oxygen partial pressure (PO_2) and/or temperature.[5, 6] One of the most important applications of OSMs is used as three-way catalysts (TWC) for the contaminant removal in automobile exhausts,[7, 8] in which the OSM helps to maintain appropriate oxygen partial pressure so that both oxidation reaction (of CO, H_2, and carbohydrates) and reduction reaction (of NOx) can occur effectively. The OSMs incorporate oxygen in higher pO_2 and release oxygen in lower pO_2, therefore for TWC, materials that can work in PSA mode (pressure swing absorption) are recommended.[7, 9, 10] For some other specific applications (e.g., Li-oxygen batteries), pure fresh oxygen gas released from oxides may be safer than that from the pressurized oxygen tank. Even though some peroxides, such as CaO_2, MgO_2, can provide fresh oxygen gas with the increase of temperature under oxidative gas, their irreversibility limits their wide applications.[11, 12] Therefore, it is important to develop special reversible OSMs which can release fresh oxygen gas with the changes of temperature under inert or oxidative atmosphere.

As a well-known structure, perovskite oxides have been recognized as one of the most important types of OSMs with excellent redox properties, high oxygen ion mobility and highly stable structure with an unusual valence state of elements or a high extent of oxygen deficiency.[13-20] Especially, those perovskite oxides based on Mn are potential OSMs because of the easy conversion between Mn^{3+} and Mn^{4+}.[21-

23] Recently, $YMnO_{3+\delta}$ has been reported to have large and reversible oxygen content at a low temperature range under oxidative atmosphere because of the easy phase transition between hexagonal $P6_3cm$ phase and more oxidized structures (e.g., $Pca2_1$, $R3c$).[24]

Brownmillerite-type perovskite oxides with a general formula of $A_2B_2O_5$ can be viewed as the anion-deficient perovskite with alternately stacked tetrahedral BO_4 and octahedral BO_6 layers.[22, 25, 26] They can uptake oxygen to form perovskite oxides $ABO_{3\pm\delta}$, thus having the potential applications as OSMs. In addition, the reversible phase change between brownmillerite-type perovskite with $A_2B_2O_5$ and perovskite with $ABO_{3\pm\delta}$ could improve the reversibility oxygen release/storage. Especially, perovskite-type oxides based on Mn have attracted remarkable attention and have been widely researched as OSMs.[27-34] For example, $BaYMn_2O_{5+\delta}$ exhibits remarkable oxygen storage capacity (OSC, 3.7 wt%) at low temperatures below 500 °C with an excellent reversible behaviour in alternative reductive (H_2) and oxidative (O_2) conditions, but it is not suitable in pure oxidative or alternative oxidative and inert gas conditions.[5, 22, 30] Thus, excellent OSMs based on brownmillerite-type perovskite oxides still need more research. Recently, $Ca_2AlMnO_{5+\delta}$ was reported to have a high OSC (~3 wt%) in response to changes in surrounding temperature and pressure of O_2 in a highly reversible behaviour, accompanied with the valence change between Mn^{3+} and Mn^{4+}.[27, 34-36] Another similar brownmillerite-type oxide, Ca_2GaMnO_5 has been investigated about its magnetic structure and oxygen content under different preparation conditions.[37, 38] Nevertheless, the detailed understanding on the phase structure and oxygen content in the solid solutions of $Ca_2(Al_{1-x}Ga_x)MnO_{5+\delta}$ is still not clear. Herein, we prepared some brownmillerite-type oxides based on $Ca_2(Al_{1-x}Ga_x)MnO_{5+\delta}$ with various substituting amounts ($0 \leq x \leq 1$),

and investigated their oxygen storage/release properties and thermal stability against temperature and the surrounding PO_2 with the purpose to better understand their oxygen storage/release mechanism.

2. Experimental Section

2.1 Synthesis

Brownmillerite-type oxides with the formula of $Ca_2(Al_{1-x}Ga_x)MnO_5$ (x = 0, 0.25, 0.5, 0.75, 1) were prepared via solid state method using $CaCO_3$, Al_2O_3, MnO_2 and Ga_2O_3 as precursors. Stoichiometric amounts of precursors were homogeneously mixed by grounding in a mortar. The obtained powders were pressed into cylindrical pellets, which were further fired in a tube furnace at 1250 ℃ under static air for 24 h and under flowing pure argon for another 12 h. Then these obtained pellets were ground into fine powder for XRD characterization and OSC test.

2.2 Characterization

Powder X-ray diffraction (XRD) patterns were obtained on a PANalytical Empyrean Reflection Diffractometer using Cu Ka radiation (λ = 1.541 Å). The oxygen uptake/release ability of these samples was tested by thermogravimetric analysis (TGA) on a NETZSCH TG 209 instrument (NETZSCH-Geraetebau GmbH, Selb, Germany) with a TASC 414/3 controller. Oxygen uptake property was obtained up to 900 ℃ with heating/cooling rates of ±1 ℃/min.

3. Results and Discussion

Fig. 1 shows the XRD patterns of as-prepared $Ca_2(Al_{1-x}Ga_x)MnO_5$ (i.e., post-annealing at 1250 ℃ under flowing argon gas for 12 h). The XRD pattern for as-prepared Ca_2AlMnO_5 in Fig. 1a can be ascribed to orthorhombic structure with *Ibm2* space group, similar to reported results.[39] The lattice parameters for as-prepared

Ca$_2$(Al$_{1-x}$Ga$_x$)MnO$_5$ after Rietveld refinement were summarized in Table 1. The lattice parameters of our as-prepared Ca$_2$AlMnO$_5$ are determined to be a = 5.4705(1), b = 15.0050(3), and c = 5.2431(1) Å.
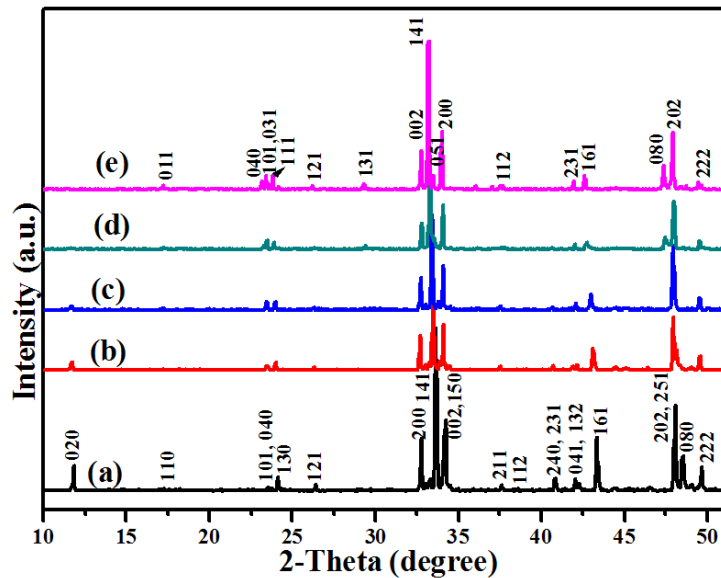
Fig. 1. XRD patterns of as-prepared Ca$_2$(Al$_{1-x}$Ga$_x$)MnO$_5$ (i.e., post-annealing at 1250 °C under flowing argon for 12 h): (a) Ca$_2$AlMnO$_5$, (b) Ca$_2$(Al$_{0.75}$Ga$_{0.25}$)MnO$_5$, (c) Ca$_2$(Al$_{0.5}$Ga$_{0.5}$)MnO$_5$, (d) Ca$_2$(Al$_{0.25}$Ga$_{0.75}$)MnO$_5$, (e) Ca$_2$GaMnO$_5$.

The XRD patterns for the as-prepared Ga-substituted samples after post-annealing at 1250 °C under Ar for 12 h can be indexed to orthorhombic structure with *Pnma* space group.[40] The crystal structures of brownmillerite-type Ca$_2$AlMnO$_5$ with *Ibm2* space group and Ca$_2$GaMnO$_5$ with *Pnma* space group are schematically shown in Fig. 2a and Fig. 2b via Diamond software,[41] respectively, based on the structure reported in literature.[37, 42, 43] As shown in Fig. 2a, Ca$_2$AlMnO$_5$ comprises tetrahedral AlO$_4$ and octahedral MnO$_6$ blocks, where the MnO$_6$ chain orientations are fully ordered.[39] As shown in Fig. 2b, the chain orientations of MnO$_6$ in Ca$_2$GaMnO$_5$ are disordered, where the R-type (right-hand chains) and L-type (left-hand chains) Ga-O chains are ordered with -L-R-L-R- alternation along the b axis.[37] The main

difference between the structures of Ca_2AlMnO_5 and Ca_2GaMnO_5 is the ordering of tetrahedron and octahedron in the orthorhombic structure, resulting in different space groups.
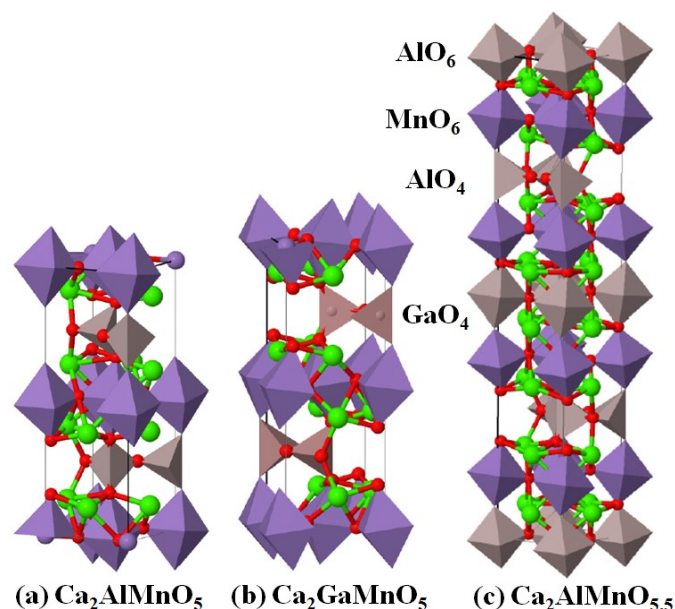
Fig. 2. Schematic illustration of the crystal structures with single cell of (a) brownmillerite-type Ca_2AlMnO_5, (b) brownmillerite-type Ca_2GaMnO_5, (c) the fully oxygenated form $Ca_2AlMnO_{5.5}$. The illustration was obtained from Inorganic Crystal Structure Database (ICSD) web and prepared via Diamond Software [41, 44] based on the structure reported in literature.[37, 42, 43]

The lattice parameters for the as-prepared $Ca_2(Al_{1-x}Ga_x)MnO_5$ in Table 1 indicate that with the increasing substitution of Ga amount ($0 < x \leq 1$), the b and c lattice parameters increased obviously and the cell volume also slightly increased, which can be attributed to the increased thickness of the $(Al,Ga)O_4$ layer due to the larger ionic radius of Ga^{3+} (0.62 Å) than that of Al^{3+} (0.535 Å). However, there is some slight decrease in the a lattice parameters with the increasing of Ga amount in the brownmillerite-type $Ca_2(Al_{1-x}Ga_x)MnO_5$ ($0 < x \leq 1.0$), which can be attributed to the tilting of the oxygen position in the MnO_6 octahedron blocks.[45, 46]

Table 1. Lattice parameters of as-prepared $Ca_2(Al_{1-x}Ga_x)MnO_5$ and oxygenated $Ca_2(Al_{1-x}Ga_x)MnO_{5+\delta}$.

| Samples	Space group	a (Å)	b (Å)*	c (Å)	Cell volume (Å^3)*	Rwp	Rp	χ^2
Ca_2AlMnO_5	*Ibm2*	5.4705(1)	15.0050(3)	5.2431(1)	430.38(2)	10.38%	7.02%	4.99
$Ca_2AlMnO_{5+\delta}$	*Imma*	5.3732(4)	14.7160(2)	5.2534(4)	415.45(1)	16.73%	11.50%	5.96
$Ca_2(Al_{0.75}Ga_{0.25})MnO_5$	*Pnma*	5.4698(2)	15.0802(6)	5.2488(4)	432.95(4)	16.26%	11.77%	6.11
$Ca_2(Al_{0.75}Ga_{0.25})MnO_{5+\delta}$	*Imma*	5.3892(2)	14.7810(1)	5.2669(2)	419.56(7)	11.34%	8.28%	2.85
$Ca_2(Al_{0.5}Ga_{0.5})MnO_5$	*Pnma*	5.4700(2)	15.1643(6)	5.2561(2)	435.99(4)	16.50%	11.76%	5.98
$Ca_2(Al_{0.5}Ga_{0.5})MnO_{5+\delta}$	*Imma*	5.4072(2)	14.8300(1)	5.2793(2)	423.35(1)	13.18%	10.38%	3.66
$Ca_2(Al_{0.25}Ga_{0.75})MnO_5$	*Pnma*	5.4617(2)	15.3012(6)	5.2629(2)	439.82(4)	16.31%	11.89%	5.87
$Ca_2(Al_{0.25}Ga_{0.75})MnO_{5+\delta}$	*Pnma*	5.4630(1)	15.1820(2)	5.2634(6)	436.60(1)	11.31%	9.15%	3.12
	Imma	5.4204(4)	14.9110(2)	5.2955(4)	428.00(1)	13.12%	10.21%	4.23
Ca_2GaMnO_5	*Pnma*	5.4611(1)	15.3303(3)	5.2664(1)	440.92(2)	15.05%	11.41%	5.00
$Ca_2GaMnO_{5+\delta}$	*Pnma*	5.4629(1)	15.3023(3)	5.2707(1)	440.61(2)	13.70%	10.27%	4.31

* b parameter and cell volume of *Imma* structure was divided by 2 to compare with those in *Ibm2* and *Pnma*

Based on the TGA test results under O_2 atmosphere (Fig. 4), all the samples obtained the highest weight at around 450 °C. Therefore, these as-prepared $Ca_2(Al_{1-x}Ga_x)MnO_5$ samples were treated in air atmosphere at 450 °C for 12 h in a furnace for oxygenation in order to check the phase structure changes of oxygenated samples. The XRD patterns of oxygenated samples are shown in Fig. 3 and their lattice parameters were also summarized in Table 1. The XRD patterns of oxygenated $Ca_2AlMnO_{5+\delta}$ (Fig. 3a) can be ascribed to the orthorhombic structure with *Imma* space group (a = 5.3732(4), b = 29.4320(2) and c = 5.2534(4) Å), similar to reported

results.[27] The crystal structure of the full oxygenated $Ca_2AlMnO_{5.5}$ is shown in Fig. 2c based on the structure reported in literature.[42] After oxygenation, the fully oxygenated $Ca_2AlMnO_{5.5}$ was composed of alternating tetrahedral AlO_4 and octahedral AlO_6 blocks, which are separated by octahedral MnO_6.[27] The structure differences between the pristine Ca_2AlMnO_5 and the oxygenated $Ca_2AlMnO_{5.5}$ imply that the oxygen uptake process mainly occur in the b-lattice direction with the partial oxidation of the tetrahedral AlO_4 to octahedral AlO_6, but still half of the AlO_4 tetrahedron are intact in the oxygenated $Ca_2AlMnO_{5.5}$, which has been considered to be linked with its reversible oxygen uptake/release process.[27] The XRD patterns of oxygenated $Ca_2(Al_{0.75}Ga_{0.25})MnO_{5+\delta}$ and $Ca_2(Al_{0.5}Ga_{0.5})MnO_{5+\delta}$ can also be ascribed to the orthorhombic structure with $Imma$ space group. In contrast, the XRD patterns of oxygenated $Ca_2(Al_{0.25}Ga_{0.75})MnO_{5+\delta}$ can be indexed to intermixed orthorhombic $Pnma$/$Imma$ space group, indicating the formation of octahedral AlO_6 blocks from tetrahedral AlO_4 blocks during the oxidation process while the GaO_4 blocks are still intact. Comparing the lattice parameters of the pristine materials (i.e., Ca_2AlMnO_5, $Ca_2(Al_{0.75}Ga_{0.25})MnO_5$, $Ca_2(Al_{0.5}Ga_{0.5})MnO_5$ and $Ca_2(Al_{0.25}Ga_{0.75})MnO_5$) and their oxygenated counterparts (i.e., $Ca_2AlMnO_{5+\delta}$, $Ca_2(Al_{0.75}Ga_{0.25})MnO_{5+\delta}$, $Ca_2(Al_{0.5}Ga_{0.5})MnO_{5+\delta}$ and $Ca_2(Al_{0.25}Ga_{0.75})MnO_{5+\delta}$), there is a large increase (a bit smaller than double) in the b lattice parameter, indicating the oxygenation reaction takes place topotactically with the formation of octahedral AlO_6 from tetrahedral AlO_4. With the increase of Ga-substituting amount ($0 \leq x \leq 0.75$) in the oxygenated $Ca_2(Al_{1-x}Ga_x)MnO_{5+\delta}$, the lattice parameters (a, b and c) and cell volumes increased due to the larger ionic radius of Ga^{3+} (0.62 Å) than that of Al^{3+} (0.535 Å). When completely substituting Al with Ga (i.e., $x = 1.0$) in $Ca_2(Al_{1-x}Ga_x)MnO_{5+\delta}$, the oxygenated $Ca_2GaMnO_{5+\delta}$ (Fig. 3e) still maintains the same orthorhombic $Pnma$ space group as

its pristine Ca_2GaMnO_5. Comparing the lattice parameters of the pristine samples (i.e., $Ca_2(Al_{0.25}Ga_{0.75})MnO_5$ and Ca_2GaMnO_5) and their oxygenated counterparts (i.e., $Ca_2(Al_{0.25}Ga_{0.75})MnO_{5+\delta}$ and $Ca_2GaMnO_{5+\delta}$) with *Pnma* space group, there are slight increases in *a* and *c* lattice parameter and obvious decrease in *b* lattice parameters, which can be attributed to the slightly compressed oxygen tetrahedra around the Ga atoms along the *b* axis during the oxidation process in air atmosphere at 450 °C for 12 h.[37, 39] However, it has been reported that oxygenated $Ca_2GaMnO_{5.39}$ can be obtained by treating Ca_2GaMnO_5 under the oxygen partial pressure of 80 atm O_2 at 415 °C for 15 h.[37] The XRD results in the pristine materials and their oxygenated counterparts indicate that Ga-substitution in $Ca_2(Al_{1-x}Ga_x)MnO_5$ would affect their oxygen uptake ability, which will be further investigated by TGA technique in following paragraphs.
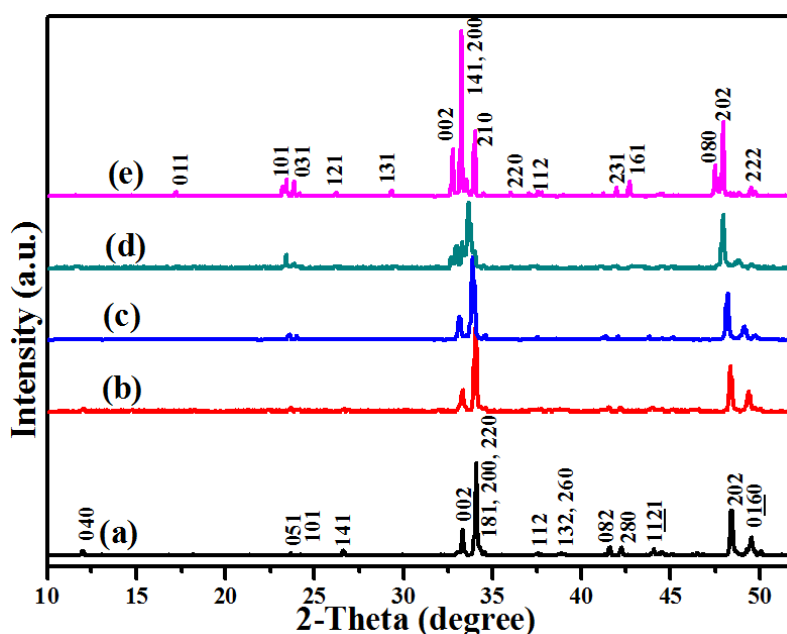
Fig. 3. XRD patterns of oxygenated samples after treated at 450 °C under static air for 12 h: (a) $Ca_2AlMnO_{5+\delta}$, (b) $Ca_2(Al_{0.75}Ga_{0.25})MnO_{5+\delta}$, (c) $Ca_2(Al_{0.5}Ga_{0.5})MnO_{5+\delta}$, (d) $Ca_2(Al_{0.25}Ga_{0.75})MnO_{5+\delta}$, (e) $Ca_2GaMnO_{5+\delta}$.

Fig. 4 shows the oxygen uptake/release properties of as-prepared samples under pure O_2 with 1 ℃/min heating and cooling rate between room temperature and 900 ℃. The results show that upon heating in O_2 atmospheres, these samples firstly remain almost stable between room temperature and 300 ℃, then sharply gain weight from 300 ℃ to reach the maximum peaks at about 370-470 ℃, which are different according to different Ga substituting amounts. The maximum weight gain (ΔW) and its corresponding temperature, OSC, oxygen content and the oxygenated samples were summarized in Table 2, in which the Mn valence in the as-prepared samples is assumed to be Mn^{3+}. $Ca_2(Al_{0.75}Ga_{0.25})MnO_5$ shows the maximum weight at 450 ℃ with a 3.16 wt% weight gain (Fig. 4b), corresponding to the OSC of 1975 $\mu mol-O \cdot g^{-1}$, while Ca_2AlMnO_5 in Fig. 4a shows the second recorded highest OSC at 370 ℃ with a 2.97 wt% weight gain, corresponding to the OSC of 1856 $\mu mol-O \cdot g^{-1}$, indicating substituting Al with 0.25 atomic Ga would improve the oxygen uptake ability maybe due to the enhanced oxygen mobility by the increased lattice parameters. It is noteworthy that even though $Ca_2(Al_{0.75}Ga_{0.25})MnO_5$ showed the highest weight increase during the initial heating process from room temperature to 400 ℃, it can't lose weight to its original value at room temperature during the consequent heating process from 550 ℃ to 900 ℃, which can be attributed to the difficulty in the transformation of octahedral GaO_6 to GaO_4 tetrahedron. Further increasing the Ga substituting amount to x ≥ 0.50 on the Al-site would result in reduced OSC, which is maybe due to the difficulty in the oxidation of GaO_4 tetrahedron in brownmillerite-type structure to octahedral GaO_6 in air atmosphere at 450 ℃, as well as the higher atomic weight of Ga than Al.[39] As a result, Ca_2GaMnO_5 in Fig. 4e can only uptake about 0.62 wt% weight gain, corresponding to the OSC of 388 $\mu mol-O \cdot g^{-1}$. It has been reported that the electron mobility to the MnO_6 layers is weakened because of

the fully filled electron orbitals of $Ga^{3+}(d^{10})$ ions.[47] As a result, the super-exchange interactions between the GaO_4 and MnO_6 layers in the brownmillerite structure are suppressed perpendicular to the octahedral MnO_6 layers.[47]
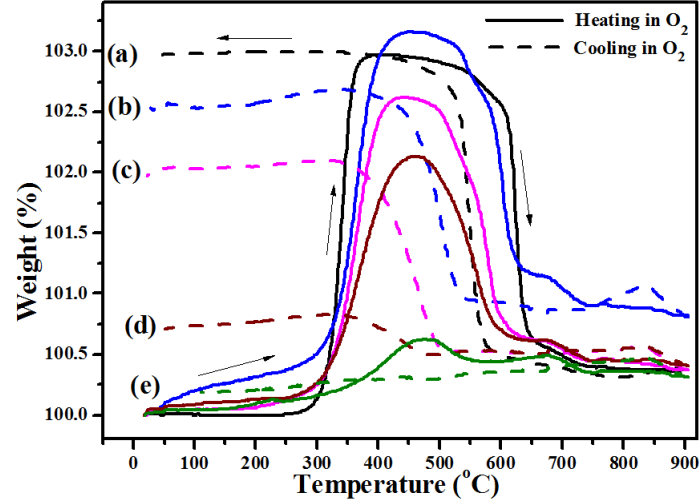
Fig. 4. TGA curves of as-prepared samples (i.e. post-annealing $Ca_2(Al_{1-x}Ga_x)MnO_5$ at 1250 °C under Ar for 12 h): (a) Ca_2AlMnO_5, (b) $Ca_2(Al_{0.75}Ga_{0.25})MnO_5$, (c) $Ca_2(Al_{0.5}Ga_{0.5})MnO_5$, (d) $Ca_2(Al_{0.25}Ga_{0.75})MnO_5$, (e) Ca_2GaMnO_5. The data were obtained under flowing O_2 with a scan rate of 1 °C/min between 20 and 900 °C.

Table 2. The maximum weight increase (ΔW), the temperature, OSC and oxygen content obtained from the oxygen uptake/release curves in Fig. 4, assuming the valence of Mn in the as-prepared samples is Mn^{3+}.

As-prepared sample	Maximum ΔW	Temperature (°C)	OSC ($\mu mol\text{-}O \cdot g^{-1}$)	Oxygen content δ	Oxygenated sample
Ca_2AlMnO_5	2.97 wt%	392	1856	0.45	$Ca_2AlMnO_{5.45}$
$Ca_2(Al_{0.75}Ga_{0.25})MnO_5$	3.16 wt%	450	1975	0.5	$Ca_2(Al_{0.75}Ga_{0.25})MnO_{5.5}$
$Ca_2(Al_{0.5}Ga_{0.5})MnO_5$	2.62 wt%	448	1637	0.43	$Ca_2(Al_{0.5}Ga_{0.5})MnO_{5.43}$
$Ca_2(Al_{0.25}Ga_{0.75})MnO_5$	2.13 wt%	452	1331	0.36	$Ca_2(Al_{0.25}Ga_{0.75})MnO_{5.36}$
Ca_2GaMnO_5	0.62 wt%	454	388	0.11	$Ca_2GaMnO_{5.11}$

Further increasing temperature would result in an abrupt weight loss at around 650 °C and plateau between 700 and 900 °C, and Ca_2AlMnO_5 shows the least weight difference with its initial value. Interestingly, during the subsequent cooling stage in flowing O_2, these samples could re-gain weight from ca. 600 °C and keep almost stable below 400 °C. In these five samples, Ca_2AlMnO_5 can almost re-gain the same weight (ca. 2.73 wt% corresponding to $\delta = 0.41$ and OSC of 1688 μmol-O$\cdot$g^{-1}) as the weight lost during the heating process. However, for the Ga-substituted samples, they can't re-gain the same weight that is lost during the heating processes. With the increasing Ga-substituting amount, the re-gained weight during the cooling process decreased, which can be attributed to the suppressed oxygen-ion mobility and desorption by the increased intact GaO_4 layers in the structure. For Ca_2GaMnO_5 shown in Fig. 4e, there is almost no weight uptake during the cooling process, which is in good agreement with its XRD results. In addition, the starting temperature for oxygen uptake during the cooling process decreased from ca. 600 °C for Ca_2AlMnO_5 to 470 °C for $Ca_2(Al_{0.25}Ga_{0.75})MnO_5$, which may be due to the different oxygen-ion mobility and distorted structure between $(Al/Ga)O_6$ and MnO_6 caused by the increased b-lattice parameter with the increasing of Ga-substituting amount. The thermal hysteresis and the differences in the TGA curves during the heating/cooling processes may be caused by their different oxygen uptake/release kinetics which is related with their composition.[27] Fig. 4 shows that the oxygen uptake/release in $Ca_2(Al_{1-x}Ga_x)MnO_{5+\delta}$ can be achieved under pure O_2 by adjusting temperature in a small range, which can be attributed to the redox equilibria of competing valence states (such as Mn^{3+}/Mn^{4+}) in the constituent transition metals,[27] similar to reported $YBaCo_4O_{7+\delta}$[48-50] and $Dy_{1-x}Y_xMnO_{3+\delta}$.[51]

Fig. 5 shows the oxygen uptake ability and OSCs of the as-prepared $Ca_2(Al_{1-}$

$_x$Ga$_x$)MnO$_5$ oxides at 450 °C under flowing O$_2$ with a 25 mL/min flowing rate. These as-prepared samples were firstly treated from room temperature to 450 °C and maintained at 450 °C for 1 h under flowing argon with 25 mL/min to remove the possible adsorbed surface oxygen species. Then, the gas was switched from argon to O$_2$ for the oxygen uptake test dependent on reaction time at 450 °C. For Ca$_2$AlMnO$_5$ and Ca$_2$(Al$_{0.75}$Ga$_{0.25}$)MnO$_5$, they uptake oxygen immediately to the maximum amount (ca. 2.73 wt% corresponding to δ = 0.41 and OSC of 1688 μmol-O·g^{-1} for Ca$_2$AlMnO$_{5.41}$, and 2.41 wt% corresponding to δ = 0.38 and OSC of 1500 μmol-O·g^{-1} for Ca$_2$(Al$_{0.75}$Ga$_{0.25}$)MnO$_{5.38}$) in 10 min. However, further increasing the Ga-substitution amount to x $\geq$ 0.5 in Ca$_2$(Al$_{1-x}$Ga$_x$)MnO$_5$ would result in less oxygen uptake in a longer time due to the lowered ionic diffusion related to the Al-O/Ga-O chemical bonds. For example, Ca$_2$(Al$_{0.5}$Ga$_{0.5}$)MnO$_5$ would uptake oxygen to the maximum amount (ca. 2.1 wt% corresponding to δ = 0.34 and OSC of 1313 μmol-O·g^{-1} for Ca$_2$(Al$_{0.5}$Ga$_{0.5}$)MnO$_{5.34}$) in about 50 min while Ca$_2$(Al$_{0.25}$Ga$_{0.75}$)MnO$_5$ needs even more time (ca. 220 min) to reach the maximum oxygen uptake amount (ca. 1.6 wt% corresponding to δ = 0.27 and OSC of 1000 μmol-O·g^{-1} for Ca$_2$(Al$_{0.25}$Ga$_{0.75}$)MnO$_{5.27}$). Ca$_2$GaMnO$_5$ can uptake only a very small amount of oxygen (ca. 0.11 wt% corresponding to δ = 0.02 and OSC of 13 μmol-O·g^{-1} for Ca$_2$GaMnO$_{5.02}$) with the increasing time to 220 min, in good agreement with their XRD patterns and lattice parameter analysis results.
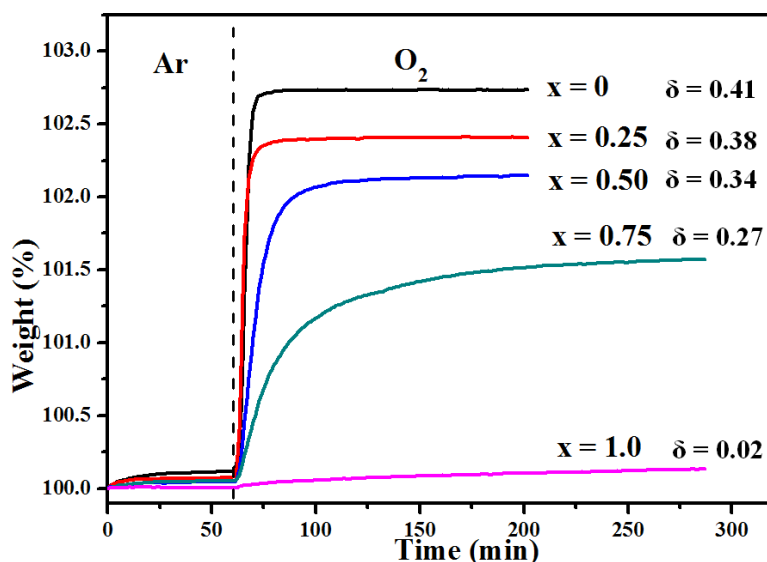
Fig. 5. Isothermal TGA curves at 450 °C for as-prepared $Ca_2(Al_{1-x}Ga_x)MnO_5$ with various x values after switching the gas flow with 25 mL/min from Ar to O_2.

As shown by the results in Fig. 4, these as-prepared samples, especially for Ca_2AlMnO_5 and $Ca_2(Al_{0.75}Ga_{0.25})MnO_5$, could change their oxygen content in a narrow temperature range (500-700 °C) under flowing O_2 atmosphere. Thus, it can be expected that remarkable oxygen uptake/release capacities can be obtained via adjusting the temperature in a small range even under pure O_2. As demonstrated in Fig. 6, a large amount of oxygen can be reversibly stored/released for Ca_2AlMnO_5 and $Ca_2(Al_{0.75}Ga_{0.25})MnO_5$ by adjusting the temperature between 500 and 700 °C. Ca_2AlMnO_5 shows a reversible and stable weight change with 2.4 wt%, larger than that of $Ca_2(Al_{0.75}Ga_{0.25})MnO_5$ with 1.9 wt%, and the results are consistent with the TGA results in Fig. 4.
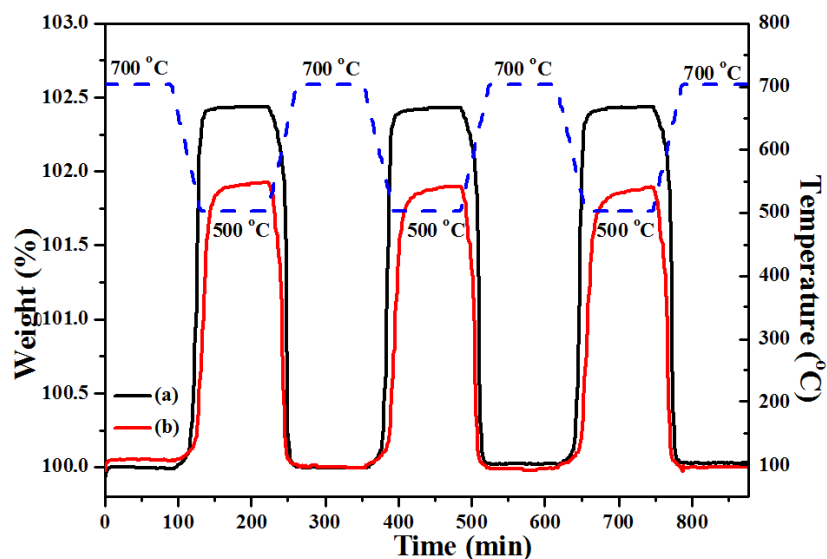
Fig. 6. TGA curves for Ca_2AlMnO_5 (a) and $Ca_2(Al_{0.75}Ga_{0.25})MnO_5$ (b) in flowing O_2 upon temperature swing between 700 and 500 °C. The sample temperature is also shown with a blue curve.

Fig. 7 shows the oxygen uptake/release cycles of as-prepared $Ca_2(Al_{1-x}Ga_x)MnO_5$ oxides at 500 °C under alternating Ar and O_2 for three cycles. The results indicate that all these five samples exhibit excellent reversibility in oxygen uptake/release via switching the gas flow between argon and O_2 at 500 °C. With the increase of Ga substituting amount from x = 0 to x = 1.0 in $Ca_2(Al_{1-x}Ga_x)MnO_5$, the total oxygen uptake/release content decreased from about 2.4 wt% for Ca_2AlMnO_5 to 0.05 wt% for Ca_2GaMnO_5. Even though the OSCs of these as-prepared samples are different, they all have good reversibility for three cycling times under inert (Ar) and oxidative gas (O_2) at 500 °C, which is important for long-term usage in practical applications.
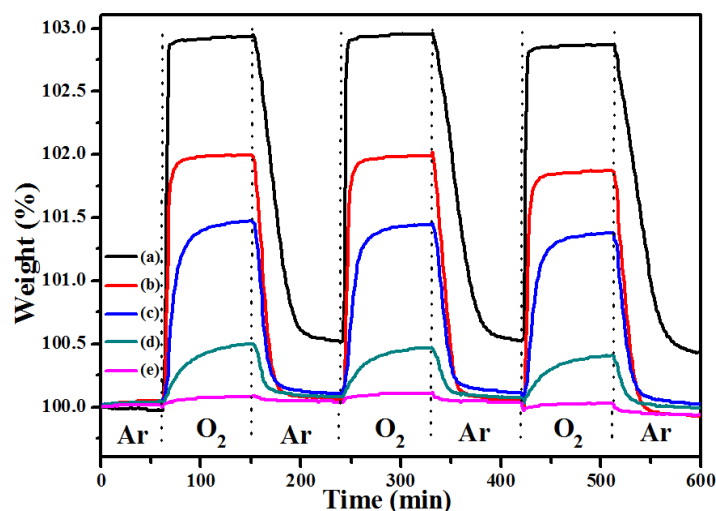
Fig. 7. TGA curves of as-prepared samples (i.e., post-annealing $Ca_2(Al_{1-x}Ga_x)MnO_5$ at 1250 °C under Ar for 12 h) obtained at 500 °C under alternating Ar and O_2 for three cycles: (a) Ca_2AlMnO_5, (b) $Ca_2(Al_{0.75}Ga_{0.25})MnO_5$, (c) $Ca_2(Al_{0.5}Ga_{0.5})MnO_5$, (d) $Ca_2(Al_{0.25}Ga_{0.75})MnO_5$, (e) Ca_2GaMnO_5.

The thermal stability of the oxygenated samples under pure argon with temperature is shown in Fig. 8. The results show that these samples are almost stable between room temperature and 400 °C under flowing argon. Further increasing temperature would result in sharp weight loss from 400 to 600 °C, and then keep stable between 600 and 900 °C. With the increasing amount of Ga, the weight loss amount between 400 and 650 °C decreased from about 2.9 wt% for $Ca_2AlMnO_{5+\delta}$ to 0.25 wt% for $Ca_2GaMnO_{5+\delta}$. The results also indicate that substituting Ga into the Al site would reduce the OSC under flowing argon, which is in good agreement with the TGA cycle test results shown in Fig. 7. As discussed in the aforementioned paragraphs, in the Ga-substituting samples, Ga would occupy the Al-site of tetrahedral AlO_4 to form GaO_4 blocks. During the oxygenation process, tetrahedral AlO_4 would transfer to octahedral AlO_6 while tetrahedral GaO_4 is very difficult to be oxygenated to octahedral GaO_6 under 1 atm O_2 conditions, therefore Ga-substituted samples would result in less OSC.
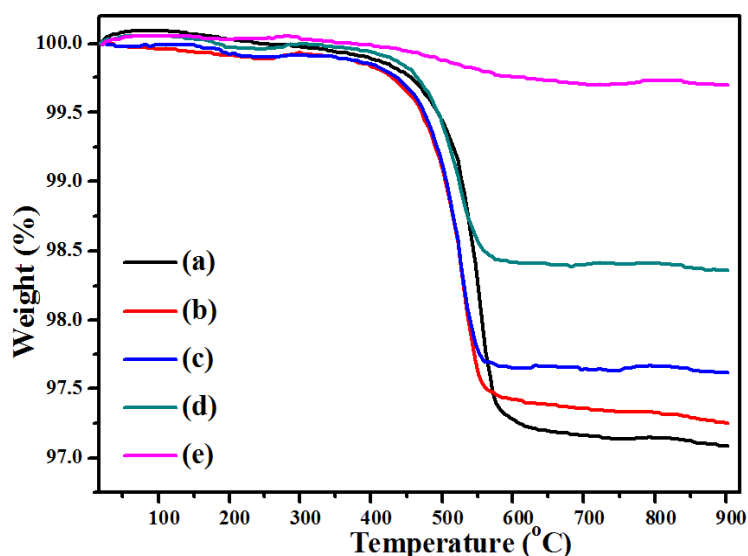
Fig. 8. TGA curves under flowing Ar of as-prepared samples after treating at 450 °C in air for 12 h: (a) $Ca_2AlMnO_{5+\delta}$, (b) $Ca_2(Al_{0.75}Ga_{0.25})MnO_{5+\delta}$, (c) $Ca_2(Al_{0.5}Ga_{0.5})MnO_{5+\delta}$, (d) $Ca_2(Al_{0.25}Ga_{0.75})MnO_{5+\delta}$, (e) $Ca_2GaMnO_{5+\delta}$. The data were measured up to 900 °C under flowing pure Ar with 10 °C/min increasing rate.

Based on the TGA results, the $Ca_2(Al_{0.75}Ga_{0.25})MnO_5$ could uptake as much as 1975 μmol-O·g^{-1} during the heating process under flowing O_2 even though its OSC in reversible test is a bit lower than that of Ca_2AlMnO_5. In addition, $Ca_2(Al_{1-x}Ga_x)MnO_5$ (x < 1) can store/release oxygen reversibly via controlling the temperature or alternating Ar and O_2. The OSCs of $Ca_2(Al_{0.75}Ga_{0.25})MnO_5$ and Ca_2AlMnO_5 are higher or comparable with the OSCs in reported results, as show in Table 3. Even though the OSCs of $YBaCo_4O_7$ and $BaYMn_2O_5$ are higher than those of $Ca_2(Al_{0.75}Ga_{0.25})MnO_5$ and Ca_2AlMnO_5 in this work, the much lower abundance and higher price of Y than those of Ca and Al would increase the cost and limit their wide applications.

Table 3. Comparison of the OSC values in this work with the reported results.

OSMs	OSC (μmol-O·g^{-1})	Temperature (°C)	Gas atmosphere	Rate (°C·min^{-1})	Ref.

$Ca_2(Al_{0.5}Ga_{0.5})MnO_5$	1975	450	O_2	1.0	This work
Ca_2AlMnO_5	1856	392	O_2	1.0	This work
$Y_{0.7}Tb_{0.3}MnO_{3+\delta}$	~770	~320	O_2	1.0	[23]
$DyMnO_3$	~810	~400	O_2	1.0	[51]
$YBaMn_2O_{5+\delta}$	~2240	~400	H_2*	1.0	[52]
$YBaCo_4O_{7+\delta}$	~2180	~400	O_2	1.0	[53]
$Ce_{1-x}Zr_xO_{2+\delta}$	360-750	~500	H_2*	-	[54]

*H_2 is used for reduction to calculate the OSC.

4. Conclusions

Several pure-phased brownmillerite-type oxides with the formula of $Ca_2(Al_{1-x}Ga_x)MnO_5$ were prepared via a solid state method. The substitution of Ga on the Al-site would result in the change of space group from *Ibm2* for Ca_2AlMnO_5 to *Pnma* for $Ca_2(Al_{1-x}Ga_x)MnO_5$ (x > 0). Substituting Al with 0.25 atomic Ga (i.e., $Ca_2(Al_{0.75}Ga_{0.25})MnO_5$) would result in improved oxygen uptake content from 1856 μmol-O·g^{-1} for Ca_2AlMnO_5 to 1975 μmol-O·g^{-1} for $Ca_2(Al_{0.75}Ga_{0.25})MnO_5$ during the heating process under flowing O_2 but less oxygen release amount during the cooling process. The $Ca_2(Al_{1-x}Ga_x)MnO_5$ (x < 1) can store/release oxygen reversibly depending on temperature between 500 and 700 °C, or alternating Ar and O_2 at 500 °C, in which Ca_2AlMnO_5 shows the highest OSC of about 2.9 wt% depending on temperature, and 2.4 wt% depending on alternative Ar and O_2 at 500 °C, as well as excellent reversibility. With the increasing of Ga-substituting amount on the Al-site, their OSC decreased to only 0.11 wt% for Ca_2GaMnO_5 which are attributed to the difficult oxidation of tetrahedral GaO_4 into octahedral GaO_6 blocks under 1 atm O_2 condition. In brief, the ability of $Ca_2Al_{1-x}Ga_xMnO_5$ OSMs to work both in pressure and temperature-controlled modes enables them great potentials in many energy-related applications.

Acknowledgements

References

[1] H. Jeen, W.S. Choi, M.D. Biegalski, C.M. Folkman, I.C. Tung, D.D. Fong, J.W. Freeland, D. Shin, H. Ohta, M.F. Chisholm, H.N. Lee, Reversible redox reactions in an epitaxially stabilized $SrCoO_x$ oxygen sponge, Nat. Mater. 12 (2013) 1057-1063.

[2] B. Bulfin, J. Vieten, C. Agrafiotis, M. Roeb, C. Sattler, Applications and limitations of two step metal oxide thermochemical redox cycles; a review, J. Mater. Chem. A 5 (2017) 18951-18966.

[3] X. Huang, C. Ni, G. Zhao, J.T.S. Irvine, Oxygen storage capacity and thermal stability of the $CuMnO_2$-CeO_2 composite system, J. Mater. Chem. A 3 (2015) 12958-12964.

[4] X. Huang, L. Liu, H. Gao, W. Dong, M. Yang, G. Wang, Hierarchically nanostructured $MnCo_2O_4$ as active catalysts for the synthesis of N-benzylideneaniline from benzyl alcohol and aniline, Green Chem. 19 (2017) 769-777.

[5] T. Motohashi, T. Ueda, Y. Masubuchi, S. Kikkawa, Oxygen intake/release mechanism of double-perovskite type $BaYMn_2O_{5+\delta}$ ($0 \leq \delta \leq 1$), J. Phys. Chem. C 117 (2013) 12560-12566.

[6] X. Huang, G. Zhao, Y. Chang, G. Wang, J.T.S. Irvine, Nanocrystalline $CeO_{2-\delta}$ coated β-MnO_2 nanorods with enhanced oxygen transfer property, Appl. Surf. Sci. 440 (2018) 20-28.

[7] J. Kašpar, P. Fornasiero, M. Graziani, Use of CeO_2-based oxides in the three-way catalysis, Catal. Today 50 (1999) 285-298.

[8] B. Guo, Effect of oxygen storage/transport capacity of nano-$Ce_{1-x}Zr_xO_2$ on far-infrared emission property of natural tourmaline, J. Alloy. Compd. 785 (2019) 1121-1125.

[9] P.S. Lambrou, A.M. Efstathiou, The effects of Fe on the oxygen storage and release properties of model Pd–Rh/CeO_2–Al_2O_3 three-way catalyst, J. Catal. 240 (2006) 182-193.

[10] M. Skoglundh, H. Johansson, L. Löwendahl, K. Jansson, L. Dahl, B. Hirschauer, Cobalt-promoted palladium as a three-way catalyst, Appl. Catal. B-Environ. 7 (1996) 299-319.

[11] Y. Ma, B.-T. Zhang, L. Zhao, G. Guo, J.-M. Lin, Study on the generation mechanism of reactive oxygen species on calcium peroxide by chemiluminescence and UV-visible spectra, Luminescence 22 (2007) 575-580.

[12] D. Golberg, Y. Bando, K. Fushimi, M. Mitome, L. Bourgeois, C.-C. Tang, Nanoscale oxygen generators: MgO_2-based fillings of BN nanotubes, J. Phys. Chem. B 107 (2003) 8726-8729.

[13] D.N. Mueller, R.A. De Souza, H.-I. Yoo, M. Martin, Phase stability and oxygen nonstoichiometry of highly oxygen-deficient perovskite-type oxides: A case study of (Ba,Sr)(Co,Fe)$O_{3-\delta}$, Chem. Mater. 24 (2011) 269-274.

[14] A. Aguadero, H. Falcon, J.M. Campos-Martin, S.M. Al-Zahrani, J.L.G. Fierro, J.A. Alonso, An oxygen-deficient perovskite as selective catalyst in the oxidation of alkyl benzenes, Angew. Chem. 123 (2011) 6687-6691.

[15] S. Inoue, M. Kawai, N. Ichikawa, H. Kageyama, W. Paulus, Y. Shimakawa, Anisotropic oxygen diffusion at low temperature in perovskite-structure iron oxides, Nat. Chem. 2 (2010) 213-217.

[16] X. Cui, R. O'Hayre, S. Pylypenko, L. Zhang, L. Zeng, X. Zhang, Z. Hua, H. Chen, J. Shi, Fabrication of a mesoporous $Ba_{0.5}Sr_{0.5}Co_{0.8}Fe_{0.2}O_{3-\delta}$ perovskite as a low-cost and efficient catalyst for oxygen reduction, Dalton Trans. 46 (2017) 13903-13911.

[17] X. Huang, J. Feng, H.R.S. Abdellatif, J. Zou, G. Zhang, C. Ni, Electrochemical evaluation of double perovskite $PrBaCo_{2-x}Mn_xO_{5+\delta}$ (x = 0, 0.5, 1) as promising cathodes for IT-SOFCs, Int. J. Hydrogen Energy 43 (2018) 8962-8971.

[18] X. Huang, G. Zhao, G. Wang, J.T.S. Irvine, Synthesis and applications of nanoporous perovskite metal oxides, Chem. Sci. 9 (2018) 3623-3637.

[19] J. Zhou, N. Wang, J. Cui, J. Wang, J. Yang, Z. Zong, Z. Zhang, Q. Chen, X. Zheng, K. Wu, Structural and electrochemical properties of B-site Ru-doped $(La_{0.8}Sr_{0.2})_{0.9}Sc_{0.2}Mn_{0.8}O_{3-\delta}$ as symmetrical electrodes for reversible solid oxide cells, J. Alloy. Compd. 792 (2019) 1132-1140.

[20] J. Wang, J. Zhou, T. Wang, G. Chen, K. Wu, Y. Cheng, Decreasing the polarization resistance of

$LaSrCoO_4$ cathode by Fe substitution for $Ba(Zr_{0.1}Ce_{0.7}Y_{0.2})O_3$ based protonic ceramic fuel cells, J. Alloy. Compd. 689 (2016) 581-586.

[21] S. Royer, H. Alamdari, D. Duprez, S. Kaliaguine, Oxygen storage capacity of $La_{1-x}A'_xBO_3$ perovskites (with A' = Sr, Ce; B = Co, Mn)—relation with catalytic activity in the CH_4 oxidation reaction, Appl. Catal. B-Environ. 58 (2005) 273-288.

[22] T. Motohashi, T. Ueda, Y. Masubuchi, M. Takiguchi, T. Setoyama, K. Oshima, S. Kikkawa, Remarkable oxygen intake/release capability of $BaYMn_2O_{5+\delta}$: Applications to oxygen storage technologies, Chem. Mater. 22 (2010) 3192-3196.

[23] A. Klimkowicz, K. Cichy, O. Chmaissem, B. Dabrowski, B. Poudel, K. Świerczek, K.M. Taddei, A. Takasaki, Reversible oxygen intercalation in hexagonal $Y_{0.7}Tb_{0.3}MnO_{3+\delta}$: toward oxygen production by temperature-swing absorption in air, J. Mater. Chem. A 7 (2019) 2608-2618.

[24] A. Klimkowicz, K. Świerczek, S. Kobayashi, A. Takasaki, W. Allahyani, B. Dabrowski, Improvement of oxygen storage properties of hexagonal $YMnO_{3+\delta}$ by microstructural modifications, J. Solid State Chem. 258 (2018) 471-476.

[25] P. Berastegui, S.G. Eriksson, S. Hull, A neutron diffraction study of the temperature dependence of $Ca_2Fe_2O_5$, Mater. Res. Bull. 34 (1999) 303-314.

[26] H. Jeen, W.S. Choi, J.W. Freeland, H. Ohta, C.U. Jung, H.N. Lee, Topotactic phase transformation of the brownmillerite $SrCoO_{2.5}$ to the perovskite $SrCoO_{3-\delta}$, Adv. Mater. 25 (2013) 3651-3656.

[27] T. Motohashi, Y. Hirano, Y. Masubuchi, K. Oshima, T. Setoyama, S. Kikkawa, Oxygen storage capability of brownmillerite-type $Ca_2AlMnO_{5+\delta}$ and its application to oxygen enrichment, Chem. Mater. 25 (2013) 372-377.

[28] S. Stober, G. Redhammer, S. Schorr, O. Prokhnenko, H. Pollmann, Structure refinements of members in the brownmillerite solid solution series $Ca_2Al_x(Fe_{0.5}Mn_{0.5})_{(2-x)}O_{5+\delta}$ with 1/2 <= x <= 4/3, J Solid State Chem. 197 (2013) 420-428.

[29] C. Ling, R. Zhang, H. Jia, Quantum chemical design of doped $Ca_2MnAlO_{5+\delta}$ as oxygen storage media, ACS Appl. Mater. Interfaces 7 (2015) 14518-14527.

[30] T. Motohashi, T. Takahashi, M. Kimura, Y. Masubuchi, S. Kikkawa, Y. Kubota, Y. Kobayashi, H. Kageyama, M. Takata, S. Kitagawa, R. Matsuda, Remarkable oxygen intake/release of $BaYMn_2O_{5+\delta}$ viewed from high-temperature crystal structure, J. Phys. Chem. C 119 (2015) 2356-2363.

[31] A. Klimkowicz, K. Świerczek, T. Rząsa, A. Takasaki, B. Dabrowski, Oxygen storage properties and catalytic activity of layer-ordered perovskites $BaY_{1-x}Gd_xMn_2O_{5+\delta}$, Solid State Ionics 288 (2016) 43-47.

[32] T. Motohashi, M. Kimura, Y. Masubuchi, S. Kikkawa, J. George, R. Dronskowski, Significant lanthanoid substitution effect on the redox reactivity of the oxygen-storage material $BaYMn_2O_{5+\delta}$, Chem. Mater. 28 (2016) 4409-4414.

[33] C. Ni, J. Ni, Z. Zhou, M. Jin, Structural and chemical stability of Sr-, Nb- and Zr-doped calcium manganite as oxygen-storage materials, J. Alloy. Compd. 709 (2017) 789-795.

[34] G. Saito, Y. Kunisada, K. Hayami, T. Nomura, N. Sakaguchi, Atomic and local electronic structures of $Ca_2AlMnO_{5+\delta}$ as an oxygen storage material, Chem. Mater. 29 (2017) 648-655.

[35] T. Motohashi, M. Kimura, T. Inayoshi, T. Ueda, Y. Masubuchi, S. Kikkawa, Redox characteristics variations in the cation-ordered perovskite oxides $BaLnMn_2O_{5+\delta}$ (Ln = Y, Gd, Nd, and La) and $Ca_2Al_{1-x}Ga_xMnO_{5+\delta}$ ($0 \le \delta \le 1$), Dalton Trans. 44 (2015) 10746-10752.

[36] T. Nomura, C. Zhu, N. Sheng, R. Murai, T. Akiyama, Solution combustion synthesis of Brownmillerite-type Ca_2AlMnO_5 as an oxygen storage material, J. Alloy. Compd. 646 (2015) 900-905.

[37] A.M. Abakumov, M.G. Rozova, B.P. Pavlyuk, M.V. Lobanov, E.V. Antipov, O.I. Lebedev, G. Van Tendeloo, D.V. Sheptyakov, A.M. Balagurov, F. Bouree, Synthesis and crystal structure of novel layered manganese oxide $Ca_2MnGaO_{5+\delta}$, J. Solid State Chem. 158 (2001) 100-111.

[38] V.Y. Pomjakushin, A.M. Balagurov, T.V. Elzhov, D.V. Sheptyakov, P. Fischer, D.I. Khomskii, V.Y. Yushankhai, A.M. Abakumov, M.G. Rozova, E.V. Antipov, M.V. Lobanov, S.J.L. Billinge, Atomic and magnetic structures, disorder effects, and unconventional superexchange interactions in $A_2MnGaO_{5+\delta}$ (A=Sr, Ca) oxides of layered brownmillerite-type structure, Phys. Rev. B 66 (2002) 184412.

[39] A.J. Wright, H.M. Palmer, P.A. Anderson, C. Greaves, Structures and magnetic ordering in the brownmillerite phases, $Sr2MnGaO_5$ and Ca_2MnAlO_5, J. Mater. Chem. 12 (2002) 978-982.

[40] A.M. Abakumov, M.G. Rozova, B.P. Pavlyuk, M.V. Lobanov, E.V. Antipov, O.I. Lebedev, G. Van Tendeloo, D.V. Sheptyakov, A.M. Balagurov, F. Bourée, Synthesis and crystal structure of novel layered manganese oxide $Ca_2MnGaO_{5+\delta}$, J. Solid State Chem. 158 (2001) 100-111.

[41] W. Pennington, DIAMOND - Visual Crystal Structure Information System, J. Appl. Crystallogr. 32 (1999) 1028-1029.

[42] H.M. Palmer, A. Snedden, A.J. Wright, C. Greaves, Crystal structure and magnetic properties of $Ca_2MnAlO_{5.5}$, an n=3 brownmillerite phase, Chem. Mater. 18 (2006) 1130-1133.

[43] M.D. Carvalho, P. Ferreira, J.C. Waerenborgh, E. Tsipis, A.B. Lopes, M. Godinho, Structure and magnetic properties of Ca2Fe1-xMnxAlO5+delta, J Solid State Chem, 181 (2008) 2530-2541.

[44] A. Belsky, M. Hellenbrandt, V.L. Karen, P. Luksch, New developments in the Inorganic Crystal Structure Database (ICSD): accessibility in support of materials research and design, Acta Crystallogr. Sect. B 58 (2002) 364-369.

[45] C. Didier, J. Claridge, M. Rosseinsky, Crystal structure of brownmillerite Ba_2InGaO_5, J. Solid State Chem. 218 (2014) 38-43.

[46] C.J. Howard, H.T. Stokes, Group-Theoretical Analysis of Octahedral Tilting in Perovskites, Acta Crystallographica Section B, 54 (1998) 782-789.

[47] J.B. Stephen, A.S. John, L.B. Michael, A.S. Christopher, P.N. Santosh, D.B. Peter, J.R. Matthew, The observation of magnetic excitations in a single layered and a bilayered brownmillerite, J. Phys. Condens. Matter. 17 (2005) 99.

[48] S. Kadota, M. Karppinen, T. Motohashi, H. Yamauchi, R-Site substitution effect on the oxygen-storage capability of $RBaCo_4O_{7+\delta}$, Chem. Mater. 20 (2008) 6378-6381.

[49] M. Karppinen, H. Yamauchi, S. Otani, T. Fujita, T. Motohashi, Y.H. Huang, M. Valkeapää, H. Fjellvåg, Oxygen nonstoichiometry in $YBaCo_4O_{7+\delta}$: Large low-temperature oxygen absorption/desorption capability, Chem. Mater. 18 (2006) 490-494.

[50] H. Hao, J. Cui, C. Chen, L. Pan, J. Hu, X. Hu, Oxygen adsorption properties of $YBaCo_4O_7$-type compounds, Solid State Ionics 177 (2006) 631-637.

[51] S. Remsen, B. Dabrowski, Synthesis and oxygen storage capacities of hexagonal $Dy_{1-x}Y_xMnO_{3+\delta}$, Chem. Mater. 23 (2011) 3818-3827.

[52] K. Jeamjumnunja, W. Gong, T. Makarenko, A.J. Jacobson, A determination of the oxygen non-stoichiometry of the oxygen storage material $YBaMn_2O_{5+\delta}$, J. Solid State Chem. 230 (2015) 397-403.

[53] O. Parkkima, H. Yamauchi, M. Karppinen, Oxygen storage capacity and phase stability of variously substituted $YBaCo_4O_{7+\delta}$, Chem. Mater. 25 (2013) 599-604.

[54] H. He, H.X. Dai, C.T. Au, Defective structure, oxygen mobility, oxygen storage capacity, and redox properties of RE-based (RE = Ce, Pr) solid solutions, Catal. Today 90 (2004) 245-254.